



Discover Generics

Cost-Effective CT & MRI Contrast Agents

**FRESENIUS
KABI**

[WATCH VIDEO](#)

AJNR

The Evaluation and Prediction of Laminoplasty Surgery Outcome in Patients with Degenerative Cervical Myelopathy Using Diffusion Tensor MRI

X. Han, X. Ma, D. Li, J. Wang, W. Jiang, X. Cheng, G. Li, H. Guo and W. Tian

This information is current as of June 29, 2025.

AJNR Am J Neuroradiol 2020, 41 (9) 1745-1753

doi: <https://doi.org/10.3174/ajnr.A6705>

<http://www.ajnr.org/content/41/9/1745>

The Evaluation and Prediction of Laminoplasty Surgery Outcome in Patients with Degenerative Cervical Myelopathy Using Diffusion Tensor MRI

X. Han, X. Ma, D. Li, J. Wang, W. Jiang, X. Cheng, G. Li, H. Guo, and W. Tian



ABSTRACT

BACKGROUND AND PURPOSE: DTI has been proved valuable for the diagnosis of degenerative cervical myelopathy, whereas its capacity for predicting the outcome of surgery is still under debate. Here we conduct a prospective cohort study to analyze the capacity of DTI for evaluating and predicting laminoplasty surgery outcome for degenerative cervical myelopathy.

MATERIALS AND METHODS: We recruited 55 patients with degenerative cervical myelopathy who underwent DTI before surgery and at 3- and 6-month follow-up stages, and 20 healthy subjects. For clinical assessment, the modified Japanese Orthopedic Association scale was recorded for each patient at different stages. DTI metrics were compared between patients before surgery and healthy subjects. Spearman correlation and receiver operating characteristic were used to analyze the evaluation and prediction capacity of DTI for the modified Japanese Orthopedic Association scale, respectively. We analyzed different vertebral levels: maximal compression level, average of all compression levels, and C2 level.

RESULTS: DTI metrics were significantly different between patients before surgery and healthy subjects. Before surgery, DTI for the maximal compression level or DTI for the average of all compression levels had no significant correlation with the modified Japanese Orthopedic Association scale. For all stages, DTI at the C2 level was correlated with the modified Japanese Orthopedic Association scale. DTI metrics at the C2 level before surgery were significantly correlated with the postoperative modified Japanese Orthopedic Association scale recovery rate. Receiver operating characteristic analysis demonstrated that fractional anisotropy at C2 was capable of predicting the postoperative modified Japanese Orthopedic Association scale recovery rate ($P = .04$).

CONCLUSIONS: The DTI metrics before laminoplasty surgery, especially fractional anisotropy at the C2 level, have the potential for evaluating and predicting the degenerative cervical myelopathy surgery outcome.

ABBREVIATIONS: AC = all compression; AD = axial diffusivity; DCM = degenerative cervical myelopathy; FA = fractional anisotropy; MC = maximal compression; MD = mean diffusivity; mJOA = modified Japanese Orthopedic Association scale; RD = radial diffusivity; ROC = receiver operating characteristic

Degenerative cervical myelopathy (DCM) is one of the most common causes of chronic spinal cord dysfunction.¹ Decompression surgery, including anterior and posterior surgery, is widely used in the treatment of DCM. However, the surgery outcome can vary among different patients. Therefore, a reliable

tool is required to evaluate and predict the surgery outcome for patients with DCM.

Noninvasive MR imaging is routinely used for the diagnosis of DCM, especially T2-weighted MR imaging, which can provide high-resolution images of anatomic structures and superior contrast in the spinal cord. In recent years, diffusion MRI² has been used for the evaluation of spinal cord function. By measuring the Brownian motion of water molecules, diffusion MR imaging can depict microstructures in living tissue. On the basis of diffusion MR imaging, DTI acquires diffusion-weighted images along multiple directions; then, quantitative

Received February 2, 2020; accepted after revision June 9.

From the Departments of Spine Surgery (X.H., D.L., J.W., W.T.) and Radiology (W.J., X.C.), Beijing Jishuitan Hospital, Beijing, China; Beijing Institute of Traumatology and Orthopaedics (X.H.), Beijing, China; Center for Magnetic Resonance Research (X.M.), University of Minnesota, Minneapolis, Minnesota; National Center of Gerontology (D.L.), Beijing, China; Center for Biomedical Imaging Research (G.L., H.G.), Department of Biomedical Engineering, School of Medicine, Tsinghua University, Beijing, China.

Xiao Han and Xiaodong Ma are co-first authors.

This work was supported by Capital's Funds for Health Improvement and Research (code CFH2020-2-1121), Beijing JST Research Funding (code ZR-201912), National Natural Science Foundation of China (code 11871459), and Beijing Jishuitan Hospital "Nova Program" (code xkxx201614).

Please address correspondence to Wei Tian, MD, Department of Spine Surgery, Beijing Jishuitan Hospital, Beijing, China, 100035; e-mail: tianweispine@163.com

Indicates open access to non-subscribers at www.ajnr.org

Indicates article with supplemental on-line tables.

<http://dx.doi.org/10.3174/ajnr.A6705>

Table 1: Summary of previous studies about prediction of DCM surgery outcome using DTI

Publications	Correlation Method	Significance	DTI Metrics	Prediction Indexes	Vertebral Levels	Surgery Method
Jones et al, 2013 ⁹	Spearman	No	FA	mJOA	MC level, C2–C3	Not specified
Wen et al, 2014 ¹⁵	Spearman	Yes	FA	mJOA recovery rate	Average of C3 to C7	Not specified
Vedantam et al, 2017 ⁵	Pearson	Yes	FA	Δ mJOA	MC level	Not specified
Maki et al, 2017 ¹⁶	Spearman	Yes	FA	Δ mJOA, mJOA recovery rate	MC level	Posterior and anterior
Kitamura et al, 2020 ¹⁷	Spearman	Yes	FA	Δ mJOA, mJOA recovery rate	MC level	Posterior
Shabani et al, 2019 ¹⁸	Intraclass correlation coefficient	Yes (–)	FA	Δ mJOA	MC level	Not specified
Iwasaki et al, 2019 ¹⁴	Pearson	No	FA	mJOA	MC level	Posterior and anterior

Note: –(–) indicates negative correlation; Δ mJOA, difference between pre- and postoperative mJOA.

metrics can be calculated, including fractional anisotropy (FA), axial diffusivity (AD), radial diffusivity (RD), and mean diffusivity (MD).

Previous studies have shown that DTI has higher sensitivity in the diagnosis of DCM compared with T2-weighted MR imaging.^{3,4} The ADC is higher and FA values are lower in patients with DCM than in healthy individuals,^{5,6} and there are significant differences between preoperation and postoperation.^{7,8} In addition, it has been shown that FA is significantly correlated with clinical assessment of the modified Japanese Orthopedic Association scale (mJOA),^{9–13} the most frequently used clinical assessment for patients with DCM.

Although DTI has proved valuable for the diagnosis of DCM, its capability for predicting the outcome of surgery is still under debate. Here, we briefly summarize the results from previous publications (Table 1). We included 7 articles studying the correlation between preoperative DTI metrics (FA) and postoperative mJOA scale, reported from 2013 to 2019. Two articles^{9,14} claimed a nonsignificant correlation, while the rest^{5,15–18} claimed a significant correlation. Note, Shabani et al¹⁸ showed a negative correlation between preoperative FA and the postoperative Δ mJOA (difference between post- and preoperative mJOA), while the other studies showed a positive correlation. Wen et al¹⁵ claimed that the mean FA value of C3 through C7 vertebral levels before surgery is significantly correlated with the postoperative mJOA recovery rate, while the FA value at the maximal compression (MC) level is not. Different correlation methods, prediction indexes, and surgery methods were adopted in these studies, which are listed in Table 1.

The purpose of this study was to further investigate the evaluation and prediction ability of DTI for the surgery outcome of patients with DCM. Specifically, only patients with posterior laminoplasty surgery with nonmetal coral implants were included. Different from practices in previous studies, we acquired DTI data not only before surgery but also at 3 and 6 months after surgery. Using the acquired data, we analyzed the difference in preoperative DTI metrics at different vertebral levels between patients and healthy subjects, the correlation between DTI and mJOA at different stages before and after surgery, and the correlation between the preoperative DTI and the postoperative mJOA recovery rate.

MATERIALS AND METHODS

Subjects and Clinical Assessment

From January 2017 to December 2017, fifty-five patients diagnosed with DCM (21 women, 35–72 years of age; mean, 58.6 ± 6.8 years) and 20 healthy subjects (6 women, 50–65 years of age; mean, 57.29 ± 5.0 years) were recruited with written consent. This study was approved by the Review Board of Research Ethics in Jishuitan Hospital. The information for all patients is summarized in On-line Table 1. The inclusion criteria were patients with DCM with the following: 1) spinal cord compression of >3 vertebral levels caused by disk herniation, ossification of the posterior longitudinal ligament, ossification of the ligamentum flavum, cervical spondylosis, or spinal canal stenosis; 2) ages from 18 to 80 years; 3) regular conservative treatment that was ineffective, with posterior cervical laminoplasty planned; and 4) no clear contraindication for surgery. The exclusion criteria were those who were not able to undergo MR imaging, had a history of spine surgery, or had injury of spinal cord or nerve root due to an operation, from which the patient was not sufficiently recovered at the final-stage follow-up.

All patients underwent posterior cervical laminoplasty with nonmetal coral implants. Therefore, no metal artifacts were expected on the MR images. Each patient was clinically assessed using the mJOA before surgery and at 3 follow-up stages: 3 months (completed in 44 patients), 6 months (completed in 37), and 1–2 years (completed in 52) after the operation. The clinical assessment was scored by 2 board-certified spine surgeons. For each patient, he or she was scored by the same surgeon at different follow-up stages.

In addition, for each patient, we calculated the mJOA recovery rate to represent the surgery outcome, defined as the following: $\text{final-stage follow-up mJOA} - \text{preoperative mJOA} / (17 - \text{preoperative mJOA}) \times 100\%$, where 17 refers to the full score of the mJOA.

MR Imaging Data Acquisition

MR imaging data were acquired on an Ingenia 3T scanner (Philips Healthcare) with a 16-channel head-neck coil. Three MR images were obtained for each patient, before surgery and at 3- and 6-month follow-up. DTI data were acquired using a single-shot EPI sequence on the axial view, with 17 slices in total

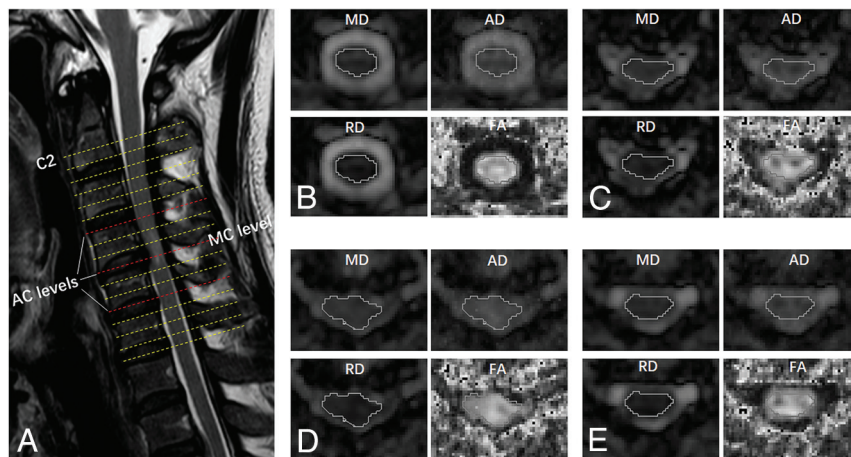


FIG 1. Example of DTI planes and ROI drawings from 1 patient. A, T2-weighted structural image with the locations of the C2 level and AC levels. B, ROI drawing at C2. C–E, ROI drawings at the AC levels. D, The MC level. Four DTI metrics were measured, including FA, AD, RD, and MD.

covering the vertebral levels from C2 to C7, shown in Fig 1. The imaging plane was parallel to the intervertebral disk at the maximal compression level. The reduced-FOV technique ($\text{FOV} = 60 \times 160 \text{ mm}^2$), outer volume suppression,^{19,20} was used to reduce image distortion, with 2 saturation bands applied at both the anterior and posterior sides to suppress foldover artifacts. Three b-values were used, $b = 0, 1000 \text{ s/mm}^2$, and 2000 s/mm^2 . The parameters were the following: number of signal averages = 1; number of diffusion directions = 32; sensitivity-encoding factor = 2; partial Fourier factor = 0.75; TE/TR = 77/4500 ms; in-plane resolution = $1.5 \times 1.5 \text{ mm}^2$; acquisition matrix size = 40×106 ; section thickness = 4 mm; section gap = 2 mm; total scan time = 5 minutes. In addition to DTI, the sagittal and axial T1-weighted and T2-weighted turbo spin-echo sequences were used for structural imaging. For each healthy subject, DTI, T1-weighted-, and T2-weighted-TSE images were acquired using the protocols identical to those of the patients. The reproducibility of DTI measurements was evaluated in our previous study,¹³ in which the percentage coefficients of variation were below 10% for all DTI metrics (Table 1 in the original article), suggesting a reliable intrascan reproducibility for them.

Image Processing

The diffusion-weighted images from the DTI data were preprocessed using the motion-correction function in the Spinal Cord Toolbox (<https://sourceforge.net/projects/spinalcordtoolbox/>)²¹ to register the images of different b-values and directions, which is a novel function that the Spinal Cord Toolbox offers with section-by-section translation estimation while ensuring regularization constraints along the section direction. Then, the DTI metrics FA, AD, RD, and MD were calculated from the registered images using the FMRIB Software Library (FSL; <http://www.fmrib.ox.ac.uk/fsl>).²² The processing steps using the Spinal Cord Toolbox and FSL were performed in Linux by batch processing without manual intervention. Afterward, the DTI metrics were loaded into DTIStudio (Johns Hopkins University)²³ in Windows and measured with ROI analysis.

For each patient, ROIs were manually drawn along the contour of the whole spinal cord at all compressed levels as well as at the C2 level containing both the white and gray matter. An example of an ROI drawing is shown in Fig 1. Specifically, the ROIs were drawn on the MD map at first and then applied to all other metrics maps because the boundary between the spinal cord and CSF can be clearly identified on the MD map. Then, the average values of all voxels inside the ROI were recorded. Note that the edge of the spinal cord was excluded from the ROI to reduce the contamination of CSF. For healthy subjects, the DTI metrics at all vertebral levels from C2 to C7 were measured using the same ROI-analysis strategy.

Statistics

Statistical analysis was performed using SPSS Statistics, Version 20.0 (IBM).

The difference in DTI metrics between the patients before surgery and the healthy subjects (control group) was analyzed using an independent 2-sample *t* test (equal variance), *t'* test (unequal variance), or Mann-Whitney *U* test. If the means of the samples were normally distributed, a *t* test or *t'* test was used; otherwise, the Mann-Whitney *U* test was used. The MC level, the average of all compression (AC) levels, and the C2 level were analyzed independently. Specifically, for the MC level, the patients were first divided into 3 groups: the MC levels at C3–4; C4–5; and C5–6 or C6–7. Then DTI was compared between each patient group and the control group (Table 2). For the average of AC levels, DTI metrics for the patients were compared with the average of C3–4 to C5–6 levels for the healthy subjects.

The Spearman correlation was used to evaluate the relationship between mJOA and DTI at the same stage (before surgery and at 3- or 6-month follow-up stages) and to evaluate the relationship between the preoperative DTI and postoperative mJOA recovery rate.

We incorporated 3 T1-weighted and T2-weighted features into a linear regression model, including the axial spinal cord area, the spinal cord flattened rate (anterior-posterior diameter of the spinal cord divided by the transverse diameter of the spinal cord), and signal changes in the T1-weighted and T2-weighted images. When we considered the influence of multicollinearity in regression analysis, each DTI metric was incorporated into the regression model separately. In other words, for each analysis, 3 traditional MR imaging metrics and 1 DTI metric were incorporated into the regression model using a stepwise linear regression strategy. The correlation was examined between the incorporated metrics and the preoperative mJOA as well as the mJOA recovery rate. The MC, AC, and C2 levels were analyzed separately.

In addition, we divided patients into 3 subgroups based on the signal changes in the T1-weighted and T2-weighted images:

Table 2: Comparison of DTI metrics between patients before surgery and the control group for the MC level

Groups/Statistics	MD ($10^{-3}\text{mm}^2/\text{s}$)		AD ($10^{-3}\text{mm}^2/\text{s}$)		RD ($10^{-3}\text{mm}^2/\text{s}$)		FA	
	Patients	Controls	Patients	Controls	Patients	Controls	Patients	Controls
Group 1 ^a	0.97 ± 0.16	0.72 ± 0.04	1.40 ± 0.11	1.35 ± 0.06	0.75 ± 0.21	0.40 ± 0.04	0.41 ± 0.14	0.66 ± 0.04
t/t' value	t' = -4.32		t' = -1.24		t' = -4.65		t' = 4.84	
P value	P = .003 ^d		P = .25		P = .002 ^d		P = .002 ^d	
Group 2 ^b	0.97 ± 0.17	0.73 ± 0.04	1.51 ± 0.16	1.32 ± 0.08	0.70 ± 0.21	0.44 ± 0.04	0.48 ± 0.14	0.61 ± 0.04
t/t' value	t' = -6.40		t' = -4.78		t' = -5.59		t' = 4.31	
P value	P < .001 ^d		P < .001 ^d		P < .001 ^d		P < .001 ^d	
Group 3 ^c	0.99 ± 0.20	0.75 ± 0.05	1.47 ± 0.15	1.26 ± 0.10	0.76 ± 0.26	0.49 ± 0.04	0.43 ± 0.16	0.55 ± 0.05
t/t' value	t' = -5.89		t' = -5.42		t' = -5.01		t' = 3.51	
P value	P < .001 ^d		P < .001 ^d		P < .001 ^d		P = .001 ^d	

^a Group 1 of patients: MC level at C3–4 (n = 8).^b Group 2 of patients: MC level at C4–5 (n = 22).^c Group 3 of patients: MC level at C5–6 or C6–7 (n = 25).^d Significant correlation.**Table 3: Comparison of DTI metrics between patients before surgery and the control group for the average of AC levels**

Groups/Statistics	MD ($10^{-3}\text{mm}^2/\text{s}$)	AD ($10^{-3}\text{mm}^2/\text{s}$)	RD ($10^{-3}\text{mm}^2/\text{s}$)	FA
Patients (n = 55)	0.87 ± 0.12	1.40 ± 0.12	0.61 ± 0.14	0.50 ± 0.10
Controls (n = 20)	0.73 ± 0.03	1.31 ± 0.07	0.44 ± 0.03	0.61 ± 0.03
t/t' value	t' = -8.19	t' = -3.15	t' = -8.36	t' = 7.10
P value	P < .001 ^a	P < .001 ^a	P < .001 ^a	P < .001 ^a

^a Significant correlation.**Table 4: Comparison of DTI metrics between the patients before surgery and the control group for the C2 level**

Groups/Statistics	MD ($10^{-3}\text{mm}^2/\text{s}$)	AD ($10^{-3}\text{mm}^2/\text{s}$)	RD ($10^{-3}\text{mm}^2/\text{s}$)	FA
Patients (n = 52)	0.74 (0.71–0.77) ^a	1.35 (1.33–1.42)	0.42 (0.39–0.47)	0.64 (0.59–0.67)
Controls (n = 20)	0.75 (0.72–0.79)	1.43 (1.33–1.48)	0.41 (0.37–0.45)	0.68 (0.64–0.70)
Z value	Z = -0.33	Z = -1.62	Z = -1.04	Z = -2.44
P value	P = .74	P = .10	P = .30	P = .02 ^b

^a Mean (lower bound-upper bound).^b Significant correlation.

patients with no signal changes (group 1), with signal changes in only T2-weighted images (group 2), and in both T1-weighted and T2-weighted images (group 3). The correlation between the DTI metrics and the preoperative mJOA or mJOA recovery rate was analyzed in each subgroup.

Receiver operating characteristic (ROC) analysis was used to evaluate the predictive capability of preoperative DTI metrics for the mJOA recovery rate. The patients were considered to have a positive recovery if the rate was >50% and to be negative otherwise. According to the positive or negative recovery, the state variables in ROC analysis were set to 1 or 0. After the ROC analysis, the cutoff value was determined to be the value with the maximum Youden index (sensitivity + specificity - 1), and the sensitivity and specificity of different DTI metrics were computed on the basis of the cutoff values.

In all statistical approaches above, the DTI metrics for the MC level, the average of AC levels, and the C2 level were analyzed independently. Due to scanning errors, the C2 level was missing on the preoperative DTI for 3 patients, so the subject size of preoperative DTI metrics at the C2 level was 52. The threshold for significance was set to .05.

RESULTS

Comparison of DTI metrics between patients before surgery with the healthy subjects is shown in Tables 2–4. For the MC level and

average of AC levels, the patients had significantly lower FA and higher MD, AD, and RD than the healthy subjects, except AD at the MC level of group 1. At the C2 level, FA was significantly lower in the patients ($P = .02$), while MD, AD, or RD had no significant difference compared with the healthy subjects.

Before surgery, Spearman correlations showed that mJOA had no significant correlation with the DTI metrics for the MC level or with those for the average of AC levels. For the C2 level, mJOA was correlated with AD ($r = 0.36$, $P = .008$), RD ($r = -0.29$, $P = .04$), and FA ($r = 0.35$, $P = .01$) (Table 5).

At the 3-month follow-up, none of the DTI metrics for the MC level had significant correlations with mJOA. At 6-month follow-up, MD, RD, and FA for the MC level were correlated with mJOA. Specifically, MD and RD showed negative correlations ($r = -0.31$, $P = .04$ and $r = -0.32$, $P = .03$, respectively), and FA showed a positive correlation ($r = 0.33$, $P = .03$) (Table 6). For the C2 level, DTI metrics had significant correlations with mJOA at both 3- and 6-month follow-up, with the detailed values listed in Table 7.

The preoperative DTI metrics for MC or the average of AC levels had no correlations with the mJOA recovery rate, while at the C2 level, AD, RD, and FA had significant correlations with the mJOA recovery rate (Table 8). Notably, FA showed the strongest correlation among the 3 metrics, with $r = 0.51$ and $P < .001$.

Table 5: Spearman correlations between the DTI metrics at different levels and mJOA before surgery

Levels/DTI Metrics	Correlation Coefficient	P Value
MC level (<i>n</i> = 55)		
MD	−0.13	.34
AD	−0.13	.34
RD	−0.07	.62
FA	−0.004	.98
Average of AC levels (<i>n</i> = 55)		
MD	−0.15	.27
AD	−0.12	.39
RD	−0.12	.38
FA	0.07	.61
C2 level (<i>n</i> = 52)		
MD	−0.09	.55
AD	0.36	.008 ^a
RD	−0.29	.04 ^a
FA	0.35	.01 ^a

^a Significant correlation.**Table 6: Spearman correlations between the DTI metrics at the MC level and mJOA at 2 follow-up stages after surgery**

Follow-Up Stages/DTI Metrics	Correlation Coefficient	P Value
3-Month follow-up (<i>n</i> = 44)		
MD	−0.12	.41
AD	−0.09	.54
RD	−0.10	.51
FA	0.10	.51
6-Month follow-up (<i>n</i> = 37)		
MD	−0.31	.04 ^a
AD	−0.14	.36
RD	−0.32	.03 ^a
FA	0.33	.03 ^a

^a Significant correlation.**Table 7: Spearman correlations between the DTI metrics for C2 level and mJOA at 2 follow-up stages after surgery**

Follow-Up Stages/DTI Metrics	Correlation Coefficient	P Value
3-Month follow-up (<i>n</i> = 44)		
MD	−0.20	.21
AD	0.16	.33
RD	−0.35	.03 ^a
FA	0.42	.005 ^a
6-Month follow-up (<i>n</i> = 37)		
MD	−0.44	.01 ^a
AD	0.15	.39
RD	−0.65	<.001 ^a
FA	0.77	<.001 ^a

^a Significant correlation.

The results of linear regression analysis incorporating DTI, T1-weighted, and T2-weighted features are shown in [Tables 9 and 10](#), where the features with significant results are listed. For the correlation with the preoperative mJOA ([Table 9](#)), only the axial spinal cord area showed significant correlation when the DTI metrics at the MC or AC levels were included, while all DTI metrics and the spinal cord flattened rate showed significant correlation when the DTI metrics at the C2 level were included. For the correlation with the mJOA recovery rate ([Table 10](#)), the DTI metrics and the spinal cord flattened rate showed significant

Table 8: Spearman correlations between the preoperative DTI metrics of different levels and the postoperative mJOA recovery rate at the final follow-up (1 year)

Levels/DTI Metrics	Correlation Coefficient	P Value
MC level (<i>n</i> = 55)		
MD	−0.10	.34
AD	0.16	.34
RD	−0.12	.62
FA	0.19	.98
Average of AC levels (<i>n</i> = 55)		
MD	−0.19	.16
AD	0.08	.59
RD	−0.24	.08
FA	0.26	.06
C2 level (<i>n</i> = 52)		
MD	−0.15	.31
AD	0.40	.003 ^a
RD	−0.42	.002 ^a
FA	0.51	<.001 ^a

^a Significant correlation.

correlation when every DTI metric at the C2 level or the FA at the AC levels was included, while only the axial spinal cord area showed significant correlation when the other DTI metrics (MD, AD, and RD at the AC levels and all DTI metrics at the MC level) were included.

For the correlation analysis in each subgroup, in group 1 with no signal changes, the AD value at the C2 level was correlated with the preoperative mJOA ($r = 0.596$, $P = .041$), and the FA value at the C2 level was correlated with the mJOA recovery rate ($r = 0.634$, $P = .027$). In group 2 with T2-weighted signal changes only, the FA value of the C2 level was correlated with the mJOA recovery rate ($r = 0.484$, $P = .042$). In group 3 with both T1-weighted and T2-weighted signal changes, the AD values of AC levels and the AD, FA, and RD values of the C2 level were correlated with the mJOA recovery rate ($r = 0.462$, 0.469 , 0.457 , and $−0.446$; $P = .03$, $.028$, $.033$, and $.037$, respectively).

The ROC analysis suggests that for the MC or average of AC levels, no DTI metrics were predictive of the mJOA recovery rate. For the C2 level, FA showed predictive capability with an area under the curve = 0.68 , $P = .04$, sensitivity = 0.56 , specificity = 0.81 ([Fig 2](#) and [Table 11](#)).

DISCUSSION

In this study, we investigated the evaluation and prediction capability of DTI for laminoplasty surgery outcome in patients with DCM. We found that DTI metrics were significantly different between patients before surgery and healthy subjects, findings consistent with those in previous studies.^{4,7,10,15} Before surgery, DTI metrics including AD, RD, and FA for the C2 level were significantly correlated with the preoperative mJOA, while DTI metrics for the MC or the average of AC levels were not. AD, RD, and FA for C2 before the operation were significantly correlated with the postoperative mJOA recovery rate. The results of regression analysis incorporating T1-weighted and T2-weighted features supported the correlation analysis results when using the DTI metrics alone, suggesting that the DTI metrics at the C2 level have the predictive value for surgery outcome. Particularly, DTI metrics were found to be correlated with the mJOA recovery rate

for each subgroup of patients on the basis of T1-weighted and T2-weighted signal changes; this correlation indicates that it is possible to define a subgroup of patients that can only be categorized using DTI alone. In addition, ROC analysis demonstrated that FA for C2 was capable of predicting the mJOA recovery rate ($P = .04$).

We obtained DTI scans for the patients with DCM before surgery and at 3- and 6-month follow-up stages. To the best of our knowledge, this was the first time that DTI data were collected at

3 different stages in the same patients with DCM. The scans at different stages helped to reveal the relationships between DTI and mJOA in a long time range and to investigate the capability of DTI in evaluating and predicting surgery outcome.

We found that before surgery, the DTI metrics for the MC level were not significantly correlated with mJOA. This was surprising because most previous studies^{5,6,9,11,15,17,18} reported significant correlation. After surgery, the DTI metrics for the MC level and mJOA were significantly correlated at 6-month follow-up, but not at 3-month follow-up.

One possible explanation is that the MC level was affected by severe image artifacts. Partial volume and motion effects could be aggravated by compression before surgery, and image distortion could be intensified by residual inflammation from surgery at 3-month follow-up, whereas at 6-month follow-up, the artifacts would be reduced so that the MC level was less affected. Other factors such as different statistical methods or patient inclusion criteria may also account for our inconsistency with previous studies.

For the C2 level, the DTI metrics were significantly correlated with the mJOA at different stages: before surgery and at 3- and 6-month follow-up. This is not surprising because it has been proved that compression might affect the distal spinal cord, even in the noncompressed regions,²⁴⁻²⁸ which may represent Wallerian degeneration that has spread from a more caudal area of stenosis.²⁹ Additionally, our results show that preoperative FA for the C2 level was correlated with the postoperative mJOA recovery rate. This correlation indicates that DTI has

Table 9: Results of linear regression to examine the correlation between DTI, T1-weighted, and T2-weighted features and preoperative mJOA

Level/Incorporated DTI Metrics	Significant Features	Slope (β)	P Value
MC level ($n = 55$)			
MD/AD/RD/FA	Axial spinal cord area	0.05	.01
Average of AC levels ($n = 55$)			
MD/AD/RD/FA	Axial spinal cord area	0.05	.01
C2 level ($n = 52$)			
MD	MD	-10.28	.03
	Spinal cord flattened rate	9.00	.005
AD	AD	5.58	.04
	Spinal cord flattened rate	6.38	.04
RD	RD	-8.93	.002
	Spinal cord flattened rate	8.32	.006
FA	FA	9.43	.002
	Spinal cord flattened rate	7.12	.02

Table 10: Results of linear regression to examine the correlation between DTI, T1-weighted, and T2-weighted features and the mJOA recovery rate

Level Incorporated DTI Metrics	Significant Features	Slope (β)	P Value
MC level ($n = 55$)			
MD/AD/RD/FA	Axial spinal cord area	0.70	.02
Average of AC levels ($n = 55$)			
MD/AD/RD	Axial spinal cord area	0.70	.02
FA	FA	108.67	.01
	Spinal cord flattened rate	105.64	.03
C2 level ($n = 52$)			
MD	MD	-157.98	.04
	Spinal cord flattened rate	141.57	.01
AD	AD	123.60	.01
RD	RD	-145.13	.004
	Spinal cord flattened rate	131.88	.01
FA	FA	170.92	.001
	Spinal cord flattened rate	111.82	.02

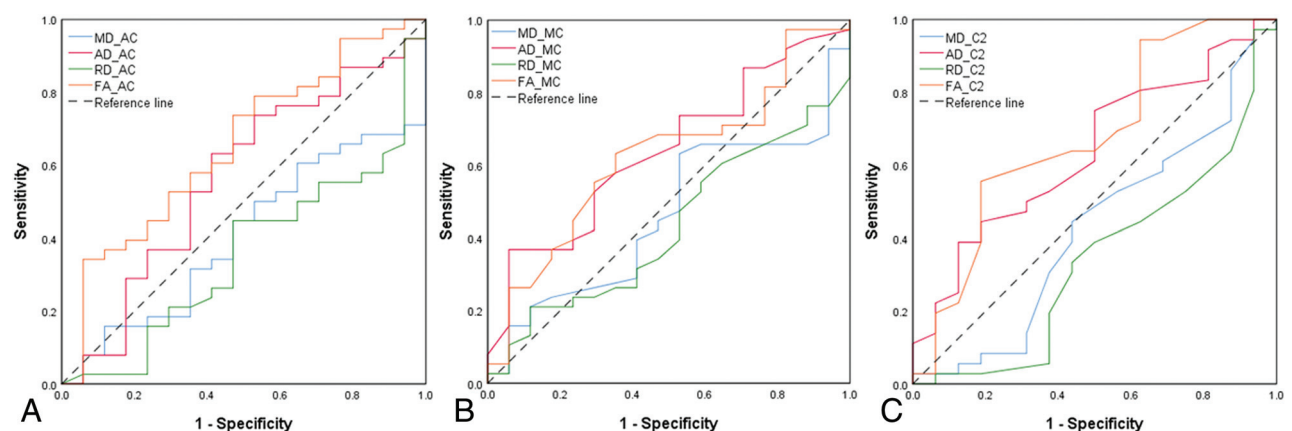


FIG 2. ROC analysis of the predictive value of DTI metrics for the postoperative mJOA recovery rate. Results for the average of all AC levels, MC level, and the C2 level, respectively. The area under the curve values for different metrics are shown in Table 11.

Table 11: Prediction capability of the preoperative DTI metrics at different levels for the postoperative mJOA recovery rate using ROC analysis

Level/DTI Metrics	AUC	P Value	Sensitivity	Specificity
MC level (n = 55)				
MD	0.46	.66	0.63	0.47
AD	0.64	.10	0.37	0.94
RD	0.43	.40	0.21	0.88
FA	0.62	.15	0.63	0.65
Average of AC levels (n = 55)				
MD	0.40	.26	0.16	0.88
AD	0.57	.43	0.63	0.59
RD	0.36	.09	0.95	0.06
FA	0.65	.07	0.34	0.94
C2 level (n = 52)				
MD	0.43	.39	0.97	0.06
AD	0.64	.12	0.39	0.88
RD	0.34	.07	0.97	0.06
FA	0.68	.04 ^a	0.56 ^a	0.81

Note:—AUC indicates area under the curve.

^a Significant correlation.

the potential to predict DCM surgery outcome. For the MC or the average of the AC levels, however, the DTI metrics were not capable of predicting the mJOA recovery rate on the basis of the data in this study. This feature may also be due to the increased artifact level caused by compression. Another possible reason is that the DTI metrics at the compression levels are affected not only by altering of the intra- and extracellular environments but also by the aligned-fiber effect. In other words, FA might be elevated to some extent if the fibers are aligned due to compression so that FA reduction resulting from spinal cord dysfunction will be compensated.¹⁴

Although most previous results reported that preoperative FA for the MC level was significantly correlated with both the preoperative and postoperative mJOA, there were several studies that reported nonsignificant correlations. Jones et al⁹ found that the preoperative FA for the MC and C2–C3 levels was correlated with the preoperative mJOA but was not correlated with the postoperative mJOA. They observed that FA at C2–C3 was more strongly correlated than at the MC level and speculated that it is due to the imaging artifacts (eg, EPI distortion) at the stenotic region, providing inconsistent DTI parameters. Wen et al¹⁵ claimed that the mean FA of C3–C7, instead of the MC level or the C2 level alone, was able to predict the postoperative mJOA. While this finding is not fully consistent with the results in this study, it provides evidence that the spinal cord function is also associated with the DTI measurements at sites distant from the MC level. Iwasaki et al¹⁴ also presented a nonsignificant correlation between the preoperative FA for the MC level and the postoperative mJOA. These studies (including the present study) have some differences in the methods, such as surgery strategy, statistics, prediction indexes, and so forth (Table 1).

To lower the image distortion, we used a reduced FOV technique, outer volume suppression, in the DTI data acquisition by applying saturation bands to suppress the signal outside the FOV along the phase-encoding direction. As shown in a previous study,³⁰ another reduced FOV technique, 2D radiofrequency

excitation, is more effective in signal suppression, though it can lead to a smaller signal strength inside the FOV than outer volume suppression. Inner volume imaging–based reduced FOV has also been applied to DTI for patients with DCM,^{31–34} which can achieve a shorter radiofrequency pulse duration compared with 2D radiofrequency excitation. However, the DTI sequence with 2D radiofrequency excitation or inner volume imaging–based reduced FOV was not available on the MR imaging system used in this study. Thus, we tried our best to optimize the outer volume suppression–based DTI on our system (3T Ingenia), including using B₁ shimming, subject-specific volume B₀ shimming, and the maximal gradient strength used for saturation. On the basis of our inspection, no obvious foldover artifacts were present on the diffusion-weighted images and calculated DTI metrics for all healthy volunteers and patients in this study. In the future, we will compare the performance difference in quantifying the spinal cord DTI metrics between outer volume suppression and 2D radiofrequency excitation when the latter is available.

As mentioned in the Materials and Methods section, the imaging plane of DTI was parallel to the intervertebral disk at the maximal compression level, which is a prescription commonly used in the previous studies. Due to the natural bending of the spinal cord, it is difficult to apply orthogonality to the nerve fibers along all cervical levels (eg, C2–C7), and the angles between the imaging plane and fiber directions may introduce bias for measuring DTI metrics. An ideal way to tackle this issue is to align the image plane of each section with the corresponding disk level through modifying the DTI pulse sequence. The viability for this modification requires investigation.

The methodology of this study had 2 major limitations. First, the diagnosis of patients included in the study was not uniform, eg, the surgical outcomes could be different between patients with ossification of the posterior longitudinal ligament and other patients with DCM, because usually the spinal cord of patients with ossification of the posterior longitudinal ligament has already been compressed for a long time; thus, their surgical outcome is relatively worse. Second, the DTI metrics of the white matter and gray matter were not analyzed separately. In this study, it is difficult to distinguish the WM and GM at the compressed levels, especially for the preoperative patients in whom the compressed spinal cord may present as only a few pixels. Even at noncompressed levels, measuring the GM and WM separately is not easy because of the limited resolution of DTI.

While we could not distinguish the WM and GM at the MC level for patients with severe compression, we were able to draw ROIs within the WM at the C2 level. For example, we drew an ROI on the dorsal column at the C2 level for all patients before surgery. The results shown in On-line Table 2 suggest that the AD of the dorsal column at the C2 level is significantly correlated with the mJOA recovery rate ($r = 0.341$, $P = .018$) and has a tendency to be correlated with the mJOA before surgery ($r = 0.264$, $P = .07$). When we used ROIs containing the whole spinal cord at the C2 level, as shown in the Results section, FA, AD, and RD were all correlated with the mJOA recovery rate. Although in theory, the spinal cord function is mainly related to WM, the ROI drawn in the dorsal column can also be contaminated by GM due to low image resolution. Additionally, the dorsal column

is a proprioceptive sensibility pathway in charge of proprioception/vibratory sense and discriminative touch, while the mJOA represents the overall sensation and motion function of the spinal cord. Furthermore, it is impractical to define the ROI of the entire WM freehand. One potential solution is to register diffusion-weighted images to the high-spatial-resolution structural images from which the GM and WM are better distinguished. We have tried to use the registration function provided by the Spinal Cord Toolbox, and it worked well for healthy subjects but failed for the preoperative patients; this outcome could be due to the influence of compression levels. Thus, a better registration algorithm is desirable for such special cases.

Overall, this study found that DTI showed the potential for predicting the mJOA recovery rate, which supports the conclusions in most previous studies. Both the Spearman correlation and ROC analysis yielded positive results for predicting the mJOA recovery rate after 1-year follow-up using the DTI metrics at the C2 level. In practice, DTI in the spinal cord inevitably faces technical limitations of spatial resolution, signal-to-noise ratio, and motion artifacts. Emerging advanced acquisition equipment such as ultra-high-field MR imaging systems³⁵ may alleviate these issues.

CONCLUSIONS

We provide a comprehensive analysis of the evaluation and prediction capability of DTI for laminoplasty surgery outcomes. Results showed that the DTI metrics at the C2 level before surgery have the potential for predicting the postoperative mJOA recovery rate.

REFERENCES

1. Tetreault L, Goldstein CL, Arnold P, et al. Degenerative cervical myelopathy: a spectrum of related disorders affecting the aging spine. *Neurosurgery* 2015;77:S51–67 [CrossRef Medline](#)
2. Basser PJ, Mattiello J, Lebihan D. MR diffusion tensor spectroscopy and imaging. *Biophys J* 1994;66:259–67 [CrossRef Medline](#)
3. Demir A, Ries M, Moonen CT, et al. Diffusion-weighted MR imaging with apparent diffusion coefficient and apparent diffusion tensor maps in cervical spondylotic myelopathy. *Radiology* 2003;229:37–43 [CrossRef Medline](#)
4. Kerkovsky M, Bednarik J, Dusek L, et al. Magnetic resonance diffusion tensor imaging in patients with cervical spondylotic spinal cord compression: correlations between clinical and electrophysiological findings. *Spine (Phila Pa 1976)* 2012;37:48–56 [CrossRef Medline](#)
5. Vedantam A, Rao A, Kurpad SN, et al. Diffusion tensor imaging correlates with short-term myelopathy outcome in patients with cervical spondylotic myelopathy. *World Neurosurg* 2017;97:489–94 [CrossRef Medline](#)
6. Ellingson BM, Salamon N, Grinstead JW, et al. Diffusion tensor imaging predicts functional impairment in mild-to-moderate cervical spondylotic myelopathy. *Spine J* 2014;24:2589–97 [CrossRef Medline](#)
7. Guan L, Chen X, Hai Y, et al. High-resolution diffusion tensor imaging in cervical spondylotic myelopathy: a preliminary follow-up study. *NMR Biomed* 2017;30 [CrossRef Medline](#)
8. Bhosale S, Ingale P, Srivastava S, et al. Diffusion tensor imaging as an additional postoperative prognostic predictor factor in cervical myelopathy patients: an observational study. *J Craniovertebr Junction Spine* 2019;10:10–13 [CrossRef Medline](#)
9. Jones JG, Cen SY, Lebel RM, et al. Diffusion tensor imaging correlates with the clinical assessment of disease severity in cervical spondylotic myelopathy and predicts outcome following surgery. *AJNR Am J Neuroradiol* 2013;34:471–78 [CrossRef Medline](#)
10. Yoo WK, Kim TH, Hai DM, et al. Correlation of magnetic resonance diffusion tensor imaging and clinical findings of cervical myelopathy. *Spine J* 2013;23:867–76 [CrossRef Medline](#)
11. Gao SJ, Yuan X, Jiang XY, et al. Correlation study of 3T-MR-DTI measurements and clinical symptoms of cervical spondylotic myelopathy. *Eur J Radiol* 2013;82:1940–45 [CrossRef Medline](#)
12. Furlan JC, Catharine Craven B. Psychometric analysis and critical appraisal of the original, revised, and modified versions of the Japanese Orthopaedic Association score in the assessment of patients with cervical spondylotic myelopathy. *Neurosurg Focus* 2016;40:E6 [CrossRef Medline](#)
13. Ma X, Han X, Jiang W, et al. A follow-up study of postoperative DCM patients using diffusion MRI with DTI and NODDI. *Spine (Phila Pa 1976)* 2018;43:E898–904 [CrossRef Medline](#)
14. Iwasaki M, Yokohama T, Oura D, et al. Decreased value of highly accurate fractional anisotropy using 3-Tesla ZOOM diffusion tensor imaging after decompressive surgery in patients with cervical spondylotic myelopathy: aligned fibers effect. *World Neurosurg* X 2019;4:100056 [CrossRef Medline](#)
15. Wen CY, Cui JL, Liu HS, et al. Is diffusion anisotropy a biomarker for disease severity and surgical prognosis of cervical spondylotic myelopathy? *Radiology* 2014;270:197–204 [CrossRef](#)
16. Maki S, Koda M, Kitamura M, et al. Diffusion tensor imaging can predict surgical outcomes of patients with cervical compression myelopathy. *Eur Spine J* 2017;26:2459–66 [CrossRef Medline](#)
17. Kitamura M, Maki S, Koda M, et al. Longitudinal diffusion tensor imaging of patients with degenerative cervical myelopathy following decompression surgery. *J Clin Neurosci* 2020;74:194–98 [CrossRef Medline](#)
18. Shabani S, Kaushal M, Budde M, et al. Comparison between quantitative measurements of diffusion tensor imaging and T2 signal intensity in a large series of cervical spondylotic myelopathy patients for assessment of disease severity and prognostication of recovery. *J Neurosurg Spine* 2019 Jun 7. [Epub ahead of Print] [CrossRef Medline](#)
19. Wilm BJ, Svensson J, Henning A, et al. Reduced field-of-view MRI using outer volume suppression for spinal cord diffusion imaging. *Magn Reson Med* 2007;57:625–30 [CrossRef Medline](#)
20. Wargo CJ, Gore JC. Localized high-resolution DTI of the human midbrain using single-shot EPI, parallel imaging, and outer-volume suppression at 7T. *Magn Reson Imaging* 2013;31:810–19 [CrossRef Medline](#)
21. De Leener B, Levy S, Dupont SM, et al. SCT: Spinal Cord Toolbox, an open-source software for processing spinal cord MRI data. *Neuroimage* 2017;145:24–43 [CrossRef Medline](#)
22. Jenkinson M, Beckmann CF, Behrens TE, et al. FSL. *Neuroimage* 2012;62:782–90 [CrossRef Medline](#)
23. Jiang H, van Zijl PC, Kim J, et al. DtiStudio: resource program for diffusion tensor computation and fiber bundle tracking. *Comput Methods Programs Biomed* 2006;81:106–16 [CrossRef Medline](#)
24. Bernabeu-Sanz A, Molla-Torres JV, Lopez-Celada S, et al. MRI evidence of brain atrophy, white matter damage, and functional adaptive changes in patients with cervical spondylosis and prolonged spinal cord compression. *Eur Radiol* 2020;30:357–69 [CrossRef Medline](#)
25. Cui L, Kong C, Chen X, et al. Changes in diffusion tensor imaging indices of the lumbosacral enlargement correlate with cervical spinal cord changes and clinical assessment in patients with cervical spondylotic myelopathy. *Clin Neurol Neurosurg* 2019;186:105282 [CrossRef Medline](#)
26. Budzik JF, Balbi V, Le Thuc V, et al. Diffusion tensor imaging and fibre tracking in cervical spondylotic myelopathy. *Eur Radiol* 2011;21:426–33 [CrossRef Medline](#)

27. Kang M, Anderer E, Elliott R, et al. **Diffusion tensor imaging of the spondylotic cervical spinal cord: a preliminary study of quantifiable markers in the evaluation for surgical decompression.** *Internet J Head Neck Surg* 2011;5. <https://print.ispub.com/api/0/ispub-article/6765>. Accessed January 15, 2019
28. Poplawski MM, Alizadeh M, Oleson CV, et al. **Application of diffusion tensor imaging in forecasting neurological injury and recovery after human cervical spinal cord injury.** *J Neurotrauma* 2019;36:3051–61 [CrossRef Medline](#)
29. Guleria S, Gupta RK, Saksena S, et al. **Retrograde Wallerian degeneration of cranial corticospinal tracts in cervical spinal cord injury patients using diffusion tensor imaging.** *J Neurosci Res* 2008;86:2271–80 [CrossRef Medline](#)
30. Wargo C, Jankiewicz M, Gore J. **Comparison of reduced FOV techniques for high resolution imaging at 7T.** *Proc Intl Soc Mag Reson Med* 2010;3012
31. Jeong EK, Kim SE, Guo J, et al. **High-resolution DTI with 2D interleaved multislice reduced FOV single-shot diffusion-weighted EPI (2D ss-rFOV-DWEPI).** *Magn Reson Med* 2005;54:1575–79 [CrossRef Medline](#)
32. Kim TH, Zollinger L, Shi XF, et al. **Quantification of diffusivities of the human cervical spinal cord using a 2D single-shot interleaved multisection inner volume diffusion-weighted echo-planar imaging technique.** *AJNR Am J Neuroradiol* 2010;31:682–87 [CrossRef Medline](#)
33. Park EH, Lee YH, Jeong EK, et al. **Diffusion tensor imaging focusing on lower cervical spinal cord using 2D reduced FOV interleaved multislice single-shot diffusion-weighted echo-planar imaging: comparison with conventional single-shot diffusion-weighted echo-planar imaging.** *Magn Reson Imaging* 2015;33:401–06 [CrossRef Medline](#)
34. Lee S, Lee YH, Chung TS, et al. **Accuracy of diffusion tensor imaging for diagnosing cervical spondylotic myelopathy in patients showing spinal cord compression.** *Korean J Radiol* 2015;16:1303–12 [CrossRef Medline](#)
35. Sigmund EE, Suero GA, Hu C, et al. **High-resolution human cervical spinal cord imaging at 7 T.** *NMR Biomed* 2012;25:891–99 [CrossRef Medline](#)